Extending the Faraday cup aerosol electrometer based calibration method up to 5 µm

Järvinen, A., Keskinen, J., and Yli-Ojanperä, J.

Aerosol Physics, Faculty of Natural Sciences, Tampere University of Technology, Tampere, Finland

Highlights:

-Electrical size classification of singly charged particles up to 5.3 µm

-Homogeneous aerosol flow splitting from 3.6 nm up to 5.3 µm with a number concentration bias less than 1 %

-Condensation particle counter calibration in the range from 3.6 nm to 5.3 µm with a single particle generator and setup

Abstract

A Faraday cup aerosol electrometer based electrical aerosol instrument calibration setup from nanometers up to micrometers has been designed, constructed and characterized. The setup utilizes singly charged seed particles, which are grown to the desired size by condensation of diethylhexyl sebacate. The calibration particle size is further selected with a Differential Mobility Analyzer (DMA). For micrometer sizes, a large DMA was designed, constructed, and characterized. The DMA electrical mobility resolution was found to be 7.95 for 20 l/min sheath and 2 l/min sample flows. The calibration is based on comparing the instrument response against the concentration measured with a reference Faraday-cup aerosol electrometer. The setup produces relatively high concentrations in the micrometer size range (over 2500 1/cm^3 at 5.3 µm). A low bias flow mixing and splitting between the reference and the instrument was constructed from a modified large sized mixer and a four-port flow splitter. It was characterized at different flow rates and as a function of the particle size. Using two of the four outlet ports at equal 1.5 l/min flow rates the particle concentration bias of the flow splitting was found to be less than ± 1 % in the size range from 3.6 nm to 5.3 µm. The developed calibration setup was used to define the detection efficiency of a condensation particle counter from 3.6 nm to 5.3 µm with an expanded measurement uncertainty (k=2) of less than 4 % over the entire size range and less than 2 % for most of the measurement points.

Introduction

Instrument calibration is one of the corner stones of reliable measurements. In the field of aerosol measurement, accurate measurement of e.g. particle number concentration is needed in clean rooms of production facilities, in ambient air monitoring and in legislated vehicle engine exhaust particulate matter emission measurements (ISO 14644-1:2015; European Commission 2008; CEN/TS 16976:2016). Calibration of an aerosol instrument in a wide particle size range is a challenging task. Firstly, the particle size range in the aforementioned applications and, consequently the measurement size ranges of common aerosol instruments extend over several orders of magnitude, from nanometers up to micrometers. Secondly, the calibration often requires monodisperse particles of known size and concentration. As a result, different particle generation and reference measurement methods are required for different size ranges (Marple et al. 1990; Marjamäki et al. 2000; Yli-Ojanperä et al. 2012; Järvinen et al. 2014). Usually the calibration of an aerosol instrument involves determination of the relationship between the measured and true values of either particle size or particle concentration. The concentration is typically expressed in terms of particle number or mass.

In some cases, the calibration of the instrument size axis is possible without the exact knowledge of the particle number concentration, e.g. in impactor calibration (Kauppinen and Hillamo 1989, Keskinen et al. 1999). If it is sufficient to calibrate instrument only for a few discrete particle sizes, traceable particle size standards may be used. Typically these are spherical polystyrene (PSL) particles, which have been characterized by microscopy, but recently, also silica particles have been introduced as a potential size standard in aerosol science (Kimoto et al. 2017). If a better size resolution than what is provided by the standard PSL spheres is needed, a different particle generation approach is required.

In sub-micrometer size range, a combination of a particle generator and a size classifier is typically used as a source of monodisperse particles. If the output size of the classifier, often a Differential Mobility Analyzer (DMA, Knutson and Withby 1975), is calibrated against traceable size standard particles, the classifier operates as a size reference in the calibration. In the micrometer size range, generators that produce monodisperse particles and for which the particle size is determined by the operating parameters, are used as a size reference. Examples of such generators are the Vibrating Orifice Aerosol Generator (VOAG, Berglund and Liu 1973) and the recent Flow-focusing Monodisperse Aerosol Generator (FMAG, Duan et al. 2016). Another option is to collect part of the calibration particles and to use microscopy as a size reference.

Unlike the calibration of the size axis, the characterization of the instrument response (detection efficiency) as a function of number concentration and/or size requires a known input concentration. At the moment, two different approaches are used as a number concentration reference in calibrations (Yli-Ojanperä et al. 2012). The first approach is a generator type Number Concentration Standard (NCS). In this case, the generator number concentration output is derived from the operating parameters, provided that the particle losses are well known or preferably insignificant. The calibration is conducted by connecting the monodisperse output of the generator directly to the inlet of the device being calibrated. The only existing generator type of NCS is the drop on demand Inkjet Aerosol Generator (IAG) of the National Institute of Advanced Industrial Science and Technology (AIST) (Iida et al. 2014), which operates in the particle size range of 0.3 and 20 µm.

The second, and the most widely applied type of NCS, is the measurement instrument approach. In this approach, a particle generator produces monodisperse particles, which are led to the device under calibration and to the reference instrument having a well-characterized detection efficiency. In sub-micrometer size range, singly charged monodisperse particles that are extracted from a polydisperse distribution with a DMA, are used in combination with a

Faraday Cup Aerosol Electrometer (FCAE) as a number concentration reference (Liu and Pui 1974; Fletcher et al. 2009; Högström et al. 2014; ISO 27891:2015). The SI-traceability for the number concentration is achieved through traceable electric current and flow rate measurements. A combination of singly charged particles and an FCAE is commonly used in measuring the counting efficiency curves of various Condensation Particle Counters (CPC) especially in the small particle sizes near the cut diameter. Multiple charging is insignificant in bipolar charging at the smallest particle diameters (Fuchs 1963; Wiedensohler 1988) and therefore mobility classification combined with FCAE enables accurate calibrations below 30 nm particle sizes. Above this, the multiple charging limits the precision. However, there are methods to limit this issue, for instance an additional aerodynamic size selection (Romay-Novas and Pui 1988; Hillamo and Kauppinen 1991; Owen et al. 2012) or modifications of the La Mer generator (Sinclair and La Mer 1948), which produce singly charged particles (Uin et al. 2009; Yli-Ojanperä et al. 2010; Yli-Ojanperä et al. 2012). In 2012, Yli-Ojanperä et al. successfully applied a modified La Mer generator and a DMA for producing singly charged calibration aerosol and for conducting a FCAE based number concentration calibration up to 1 µm. Provided that the modified La Mer generator is capable of producing particles larger than 1 µm, the upper size limit of this calibration method could be increased by constructing a larger DMA. A new DMA is needed because conventional DMAs operated at very low polydisperse and sheath flow rates, 0.2 l/min and 2.0 l/min respectively, can classify singly charged particles only up to approximately 1 µm. In a CPC calibration, the total output flow rate required by the CPC and the reference instrument is usually 2 l/min or larger. Therefore, the DMA output flow of 0.2 l/min is diluted by a factor of 1/10, which results in a low output number concentration. By operating the DMA with lower than standard sheath flow rate, it is possible to extend the size range a little (e.g. Järvinen et al. 2014; Yli-Ojanperä et al. 2014), but when high flow and relatively high number concentration of monodisperse particles are required, a large size DMA (e.g. Uin et al. 2011) becomes essential.

In principle, the available calibration methods cover the entire size range from nanometers up to micrometers but the calibration concentrations and the availability of the calibration methods, especially in the micrometer range are very limited. So far, the only published traceable number concentration standard in the micrometer size range with uncertainty less than 5 % is the IAG of AIST, which is limited to an approximately 50 1/cm^3 number concentration (Iida et al. 2014). A calibration method producing higher number concentrations in the micrometer size range, which has not been available, would be useful in CPC and Optical Particle Counter (OPC) calibrations, and especially useful in calibrations of charger-based instruments, such as the Electrical Low Pressure Impactor (ELPI, Keskinen et al. 1992, Marjamäki et al. 2000, or ELPI+, Järvinen et al. 2014).

Micrometer sized particles are affected by inertial deposition in the bends of the flow channel. In calibration applications, flow splitters potentially induce particle losses due to inertial deposition (e.g. Gupta and McFarland 2001). Uneven particle losses between the flow splitter ports result in a concentration bias between the instrument under calibration and the reference. This bias might be significant both for the smallest nanoparticles and for micrometer sized particles, easily up to several percent in some cases (Li et al. 2014). Bias values of this magnitude are unwanted and need to be compensated, which is not an easy task. Compensation of high bias values using calculated correction factors is neither a good practice nor does necessarily provide correct results. In addition, the bias depends on particle size and flow rates. Thus, the concentration bias should be minimal and experimentally evaluated. The procedure for the evaluation of the bias is presented e.g. in Yli-Ojanperä et al. (2012) and in ISO 27891:2015.

In this study we introduce a new Faraday cup aerosol electrometer based instrument calibration setup utilizing singly charged particles, a new custom made large particle DMA and

a carefully designed low particle bias flow mixing and splitting setup. The size range of the calibration setup ranges from nanometers up to micrometers. To verify the operation of the new calibration setup, we characterize the particle generator output, the large DMA transfer function, and how well the calibration aerosol can be divided between the instrument under calibration and the FCAE acting as a reference, i.e. the bias of the flow splitting. Finally, the potential of the developed setup is demonstrated by determining the counting efficiency of a CPC in the size range from 3.6 nm up to 5.3 µm.

Calibration setup

The developed aerosol instrument calibration setup is a modification of a setup previously introduced by Yli-Ojanperä et al. (2012). The particle generation scheme follows the principle by Uin et al. (2009) used in the Single Charged Aerosol Reference (SCAR, Yli-Ojanperä et al. 2010). In this case, we have taken the SCAR (Yli-Ojanperä et al. 2010; Högström et al. 2011; Yli-Ojanperä et al. 2012) as our basis, which is further developed for larger µm-sized particles, by developing a new particle growth unit to withstand higher temperatures, a new DMA to classify larger particles as well as a new flow mixing and splitting setup to provide equal output concentrations also in the µm-sizes. These developments are discussed in more detail after the general description of the setup.

General description of the setup

The particle generation setup is shown in Figure 1A along with different measurement configurations. The particle generation resembles the principle of the La Mer generator (Sinclair and La Mer 1948), where small primary particles are grown by condensable material, in this case diethylhexyl sebacate (DEHS). As a first stage in the setup, the primary aerosol is generated by introducing a nitrogen flow of 2.5 l/min into a tube furnace containing silver at 1180 °C temperature. After the furnace, cooling initiates nucleation of silver resulting in an approximately 10 nm particle mode. This primary aerosol is further diluted with nitrogen and a flow of 2 l/min is taken for the following stages. In addition to dilution flow adjustment, a dilution bridge is used to control the concentration. The silver particles are then charge conditioned in a Kr-85 neutralizer (Model 3077A, TSI Inc.). Because the particles are small, approximately 10 nm, the particles receive only a single elementary charge, positive or negative, or they are neutral. The fraction of particles with multiple elementary charges is minimal. The positively charged 10 nm particles are selected in a DMA (Model 3085, TSI Inc.), which is operated in a closed sheath flow loop configuration, sheath 20 l/min and sample 2 l/min. The seed particles are then introduced into a particle growth unit, which grows particles with DEHS to the desired size (a more detailed description is given later). In the original SCAR, the particle sizes were smaller and homogenous nucleation of the DEHS could be mostly avoided (Yli-Ojanperä et al. 2010). As micrometer sized particles are produced by condensation, the high DEHS vapor concentration results in homogenous nucleation. These nucleated particles are neutral and they are removed by a second DMA.

The second DMA removes the neutral nucleated particles and also enables particles/no particles signal, which is used to compensate the electrometer zero level in calibration measurements. In the developed setup, the particle size ranges from approximately 3.0 nm (if the silver primary distribution is used) up to 5.3 µm, and cannot be covered by a single DMA.

Thus, three different DMAs are used, one at a time. The smallest particles, up to 40 nm, are classified using a nano-DMA (Model 3085, TSI Inc.). In the size range between 40 and 250 nm a medium length Vienna type DMA with a 280 mm long classification section is used. The particle sizes above 250 nm are classified with the new large DMA: Tampere Long DMA, described later in more detail.

After the DMA, the flow rate of the calibration aerosol is matched with the instruments by diluting or by removing the extra flow. Then, pressure, temperature and humidity are measured from the line with a PTH-sensor (PTU303, Vaisala Oyj) and the flow is introduced into a mixer followed by a flow splitter, see more detailed description later. The outlets of the flow splitter are connected to the instrument and the FCAE reference. The FCAE consist of a Faraday-cup filter and an electrometer (Model 6430, Keithley). The FCAE flow rate is controlled with a mass flow controller (Model MC-2SLPM-D/5M, Alicat Scientific Inc.).The SI-traceability for the number concentration in the calibration setup is achieved through traceable electric current and flow rate measurements.

Particle growth unit

A new particle growth unit was developed to facilitate the production of higher DEHS concentrations required for growing the particles to µm-sizes. The singly charged primary aerosol is introduced into a saturator, where the gas is saturated with DEHS. The saturator is a ceramic wick installed inside a heated stainless steel tube and impregnated with DEHS. The saturator is surrounded by a heating element and temperature is measured with a thermocouple and adjusted with a dedicated controller (E5GN, Omron). The saturator temperature controls the output particle size. The flow cools down to room temperature in a condenser, which is a 1 m long vertical tube with 10 mm outer and 8 mm inner diameter. When the flow cools, DEHS condenses on the singly charged silver primary particles resulting in the singly charged calibration aerosol. The DEHS vapor condenses on all available surfaces including the walls of the condenser. To avoid excessive amounts of liquid DEHS coming from the outlet, the calibration aerosol is taken from the middle of the condenser, while the DEHS from the walls is collected into a separate bottle.

Tampere Long DMA

Because the singly charged micrometer-sized particles have extremely low electrical mobilities, the conventional DMAs cannot classify these particles if the DMAs are operated with high sample and sheath flows. To overcome this issue, a large sized DMA was constructed. The Tampere Long DMA consist of a tangential particle inlet, similar to Vienna DMAs (Winklmayr et al. 1991), followed by a 1.7 m long classification section with 72 mm inner and 80 mm outer radius. The flow channels are rounded to minimize large particle losses. Aluminum was chosen as a main construction material because it is easily machined, lightweight and adequately resists corrosion. In addition, aluminum precision cylinder tubes are available, and the outer tube was constructed from this type of tube. The electrical insulators are made of polyethylene, which is a combination of decent mechanical properties and a good chemical resistance. The chemical resistance is required because significant amounts of DEHS enter the DMA because of the large particle size. The advantage of the DEHS as a particle material is that it dissolves into ethanol and 2-propanol. The DMA was designed so that the cleaning is as easy as possible by opening the upper part of the DMA and flushing the internal parts with the solvent, 2-propanol or ethanol, which is then collected into a bottle from the excess and monodisperse outlets. The solvent is then dried by flushing

the DMA with clean air or nitrogen. For singly charged particles, the maximum classified particle sizes are approximately 2.5 µm and 5.3 µm at 20 l/min and 10 l/min sheath flow rates.

The commonly used calculation of the DMA outlet mobility (Knutson and Whitby 1975) does not include gravity, which produces slow downward velocity especially at micrometer sizes. As the calibration sizes are extending into micrometers, gravity was taken into account. The effect of gravity is corrected using a method where the particle terminal velocity due to gravity is added to the velocity resulting from the flow rate (Uin et al. 2011). The effect of gravity is rather small, less than 2 % for the particle size of 5.3 µm at 10 l/min sheath flow.

Mixer and flow splitter

An equal particle concentration is required for both the reference and the instrument under calibration. This may be challenging for the smallest particles and especially for large µm-sized particles (Li et al. 2014). One option to ensure equal concentrations after flow splitting is to use a static flow mixer before the flow splitter (e.q. Yli-Ojanperä et al, 2012). For coarse particles, high flow velocities in sharp turns cause inertial deposition. This can be avoided with a large cross-sectional area and long mixing element length. For the new setup, a large sized 12 element stainless steel static mixer (FMX8412S, Omega Engineering Ltd.) was selected. This was modified by inserting a conical piece inside after the mixing elements to minimize particle losses. The static mixer is followed by a 280 mm long tube (15.7 mm inner diameter) to stabilize the flow before the 4-port flow splitter (Model 3708, TSI Inc.). The FCAE and the instrument under calibration are connected symmetrically to the flow splitter with 6 mm outer and 4 mm inner diameter stainless steel tubing with equal length and bending radius.

Characterization of the calibration setup

A variety of test measurements were conducted to evaluate the new components of the developed calibration setup including the particle growth unit output, transfer function of the Tampere Long DMA, as well as mixer and flow splitter bias. Furthermore, the setup was used to calibrate the detection efficiency of a CPC in the size range between 3.6 nm and 5.3 µm. All measurement configurations used in this study are presented in Figure 1.

Particle growth unit

The particle growth unit was characterized with 2 l/min flow rate, which is the same as the outlet flow of the DMA classifying silver primary particles. The objective was to find the relationship between the outlet size distribution and the saturator temperature. In this case, the focus was on larger particles, and the growth unit was studied in the size range from 350 nm to 5.3 µm. The measurement setup for the growth unit characterization is presented in Figure 1B. The size distributions were measured with the Tampere Long DMA by scanning the classifying voltage over the size distribution and measuring the concentration by a CPC (Model 3776, TSI Inc.). The response of this CPC 3776 was defined in the corresponding size range against the FCAE and the results were used to correct the CPC readings.

DMA transfer function

The DMA transfer function can be tested with monodisperse particles of a known charge level. The concentration of 1 µm size standard particles (Product number 72938, Sigma-Aldrich Inc.), atomized from ultra-pure water solution, and charge conditioned in a neutralizer was applied as a first attempt, but the resulting number concentration was too low for analyzing the transfer function. However, these size standard particles were used to check that the calculated DMA size matched the standard size, which was the case. Higher concentrations were achieved by measuring the transfer function of the Tampere Long DMA with monodisperse 400 nm singly charged DEHS particles. These particles were generated using the developed particle growth unit. Because the distribution from the growth unit is not monodisperse, a DMA (Model 3071, TSI Inc.) was used to select a narrow size range after the growth unit as illustrated in Figure 1C. This DMA was operated with 6 l/min sheath and excess flows in addition to 0.3 l/min sample and monodisperse flows. This flow ratio of 20 produces a narrow size distribution, which simplifies the calculation of the transfer function. The particle concentrations were monitored with 2 CPCs (both Model 3776, TSI Inc.), one before the Long DMA and one after the Long DMA. Both CPCs were operated with 1.5 l/min sample flows. Additional dilution and excess flows were used to balance the DMA sample flow to 2 l/min. The measurement of the transfer function was conducted by scanning the Long DMA voltage over the monodisperse size distribution. Transfer function was measured with 20 and 10 l/min sheath flow rates while the sample flow was maintained at 2 l/min.

Mixer and flow splitter tests

The flow splitting was studied with two identical FCAEs, by measuring the concentration bias between the two FCAEs as presented in Figure 1D. Equal flow rates were drawn through these FCAEs, using mass flow controllers (MC-2SLPM-D/5M and MC-5SLPM-D/5M, Alicat Scientific Inc.) and both mass flow controllers were calibrated with the same separate flow meter (M-2SLPM-D/5M, Alicat Scientific Inc.) to ensure maximum accuracy. The electric currents from the FCAE Faraday-cup filters were measured with a multichannel electrometer (ELPI, Dekati Ltd.). The two electrometer channels of the ELPI used in the electric current measurements were calibrated with the same electric current calibrator.

The most challenging cases in the flow splitting are the smallest and the largest particle sizes. The smallest particles are prone to diffusion losses and the largest particles are prone to inertial losses. Because the inlet tubing (length and bending radius) and the flow rates for the device under calibration and for the reference instrument are identical, the bias due to diffusion losses should not depend on the absolute flow rate as far as the flows stay laminar. In this study, the FCAE flow rates are between 0.50 and 2.00 l/min. Consequently, the flows remain laminar as the maximum Reynolds number is 710. Bias due to inertial losses on the other hand may change noticeably due small differences of any kind in the flow lines. Therefore, the flow splitter bias was characterized using the largest easily produced particle size of 5.3 µm at different flow rates. In addition, the flow splitting was characterized for the CPC calibration setup as a function of particle size at the same size range used in the CPC calibration and at the same 1.5 l/min flow rate.

CPC calibration

The developed setup was applied in the calibration of a CPC (Model 3775, TSI Inc.) from 3.6 nm up to 5.3 µm using the setup illustrated in Figure 1E. Both the CPC and the FCAE were operated at 1.5 l/min flow rate. The lowest size range was covered by the silver primary particles ranging from 3.6 nm to 15 nm. The growth unit was used for particle sizes above 15

nm. The 15 nm size was measured with both silver and DEHS particles to see if there was a difference between the two particle materials. The entire size range is too wide to be covered with a single DMA. Thus, a set of 3 different DMAs was used for the size ranges that were presented in the Calibration setup section earlier. The DMAs were operated with 2 l/min sample and 20 l/min sheath flows in a closed loop configuration, except the largest particle sizes above 2.5 µm, where the sheath flow was reduced to 10 l/min. The same high voltage power supply (HCP 1,25-12500 MOD, FuG Elektronik GmbH) was used with all three DMAs. The reference particle concentration was adjusted between 4000 and 14000 1/cm^3. For the two smallest and the largest particle sizes, this concentration level was not reached and the concentrations were slightly lower. Each measurement point consisted of 2 min particle measurement period repeated for 10 times. The particle free period to check the electrometer zero level was maintained for 2 min between the particle measurement periods and before and after the entire sequence. From these 2 min periods, 1 min was used to wait for stabilization and 1 min was used to calculate the average electric currents.

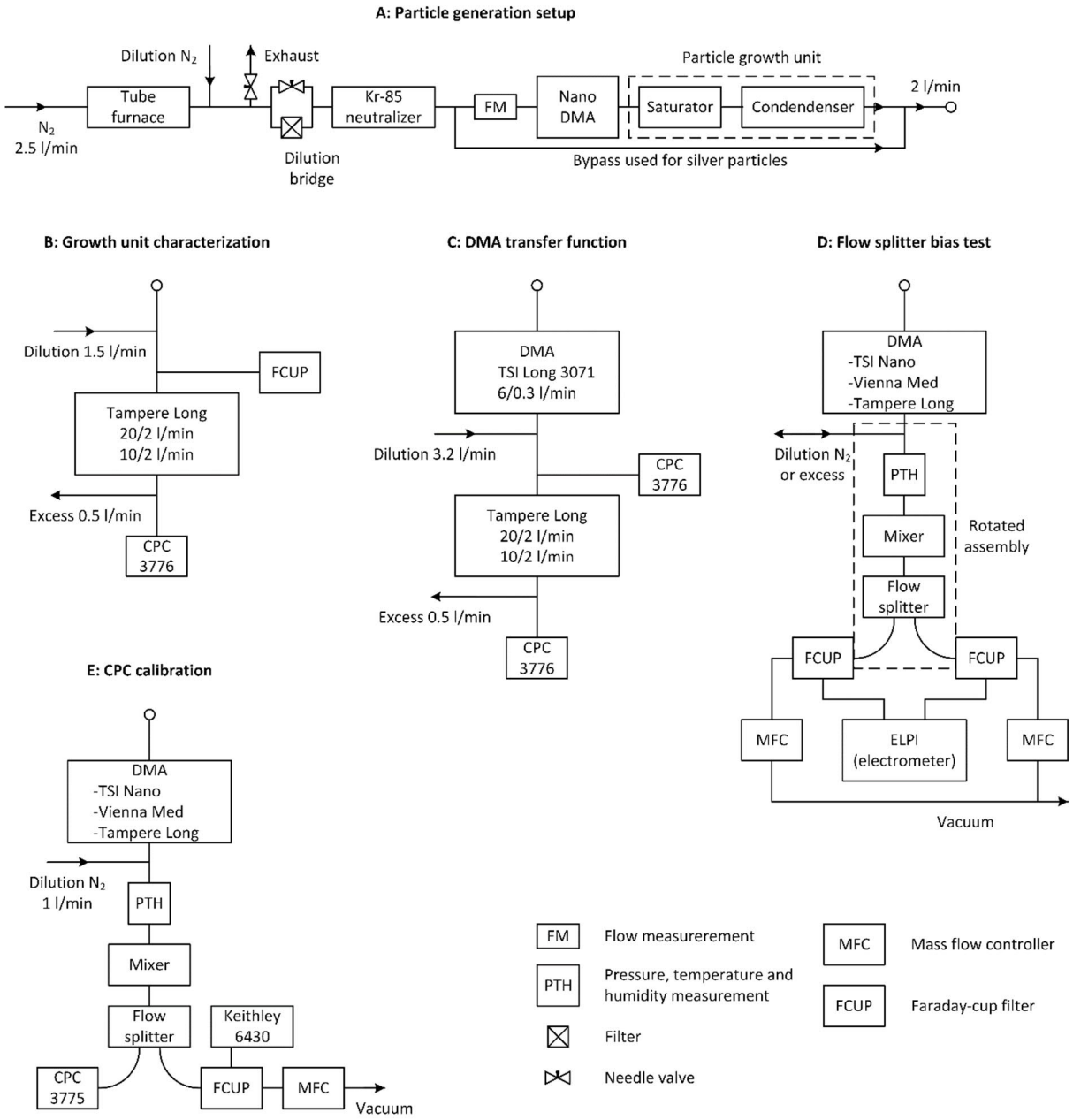

Figure 1. Measurement setups. The particle generation setup (A) remained the same during all measurements. The instrument setups (B-E) were varied depending on the measurement interest. Setup (B) was used to characterize the particle growth unit, (C) the DMA transfer function, (D) the flow splitter bias, and (E) was used in the CPC calibration.

Results and discussion

Particle growth unit

The growth unit operation was tested as a function of the saturator temperature. The outlet particle size distributions for different saturator temperatures are shown in Figure 2 including 2-part Gaussian fits. In this case particles were detected with a calibrated CPC. The CPC counting efficiency decreases over 2 µm particle sizes, which is corrected in the figure. The growth unit also works at lower temperatures but the distributions are not shown here as the main focus is on µm-sized particles. The output concentration remains high up to a saturator temperature of 190 °C, producing approximately 1.5 µm particles, but decreases above this. The concentration increase at 210 °C temperature in Figure 2 is observed because between 190 and 210 °C temperatures the first stage dilution was minimized to maximize the output concentration. Note that in Figure 2 the y-axis is the measured number concentration, which also represents the maximum possible concentration when the setup is used to calibrate instruments in the case of the three largest sizes when the primary dilution was minimized. The concentration could be increased if the distance between the first DMA and the saturator was shortened to minimize seed particle losses or if the particle generation could be located above the DMA. In current setup, particles are subjected to gravitational losses as they are brought from the level of the laboratory table up to the DMA inlet close to the ceiling.

The modal diameters from the fits are shown as a function of the saturator temperature in Figure 2. The fit predicts a steady increase in particle diameter for increased saturator temperature. However, in practice, the particle diameter levels and does not increase above 260 °C temperatures limiting the particle diameter to approximately 5 to 6 µm. The growth unit produces particle distributions with geometric standard deviations within 1.10 and 1.17 in the tested size range.

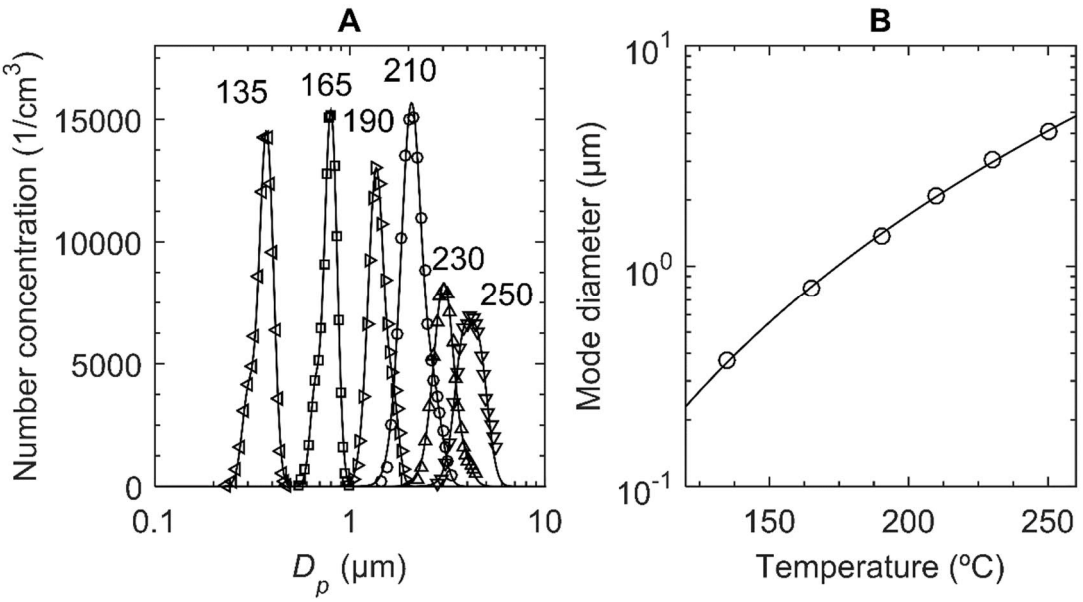

Figure 2. Growth unit size distributions for different saturator temperatures (°C) (A) and mode diameters as a function of temperature (B). The symbol D_p refers to the particle mobility diameter.

DMA transfer function

The DMA transfer function was tested using singly charged DEHS particles, which were first classified with a commercial DMA (Model 3071, TSI Inc.) operated with 6 l/min sheath and 0.3 l/min sample flows. Because of the narrow input distribution and constant concentration at inlet of the Tampere Long DMA, the transfer function was calculated straight from the CPC concentration measured after the Tampere Long DMA. The transfer function for 20 l/min and 10 l/min sheath flows in conjunction with 2 l/min sample flows is shown in Figure 3 including 2-part Gaussian fits. In the case of the 20 l/min sheath, the transfer function width (Full Width Half Maximum, FWHM) is $0.434 \cdot 10^{-9}$ m^2/Vs and the peak mobility is $3.45 \cdot 10^{-9}$ m^2/Vs producing resolution of 7.95. The obtained resolution value for 20/2 flow configuration is somewhat lower than the theoretical maximum of 10. However, the obtained resolution value is acceptable for a large DMA compared to previous devices. For instance, Uin et al. (2011) reported a β-value of 0.17 for a large sized DMA, which corresponds a resolution of 5.88. The measured transfer function differs in some degree from the typical triangular shape, especially at the lower mobilities. The reason for this difference is unknown, but it may originate from small deviations from the design values, especially in terms of concentricity. For the 10 l/min sheath flow the width increases as expected, and is $0.767 \cdot 10^{-9}$ m^2/Vs, while the peak mobility is $3.42 \cdot 10^{-9}$ m^2/Vs. These values produce resolution of 4.45, which is closer to the theoretical maximum of 5 for this 10/2 flow configuration. The transfer function resembles the triangular shape in this case, indicating that the width of the transfer function originates more from the flow configuration than other factors.

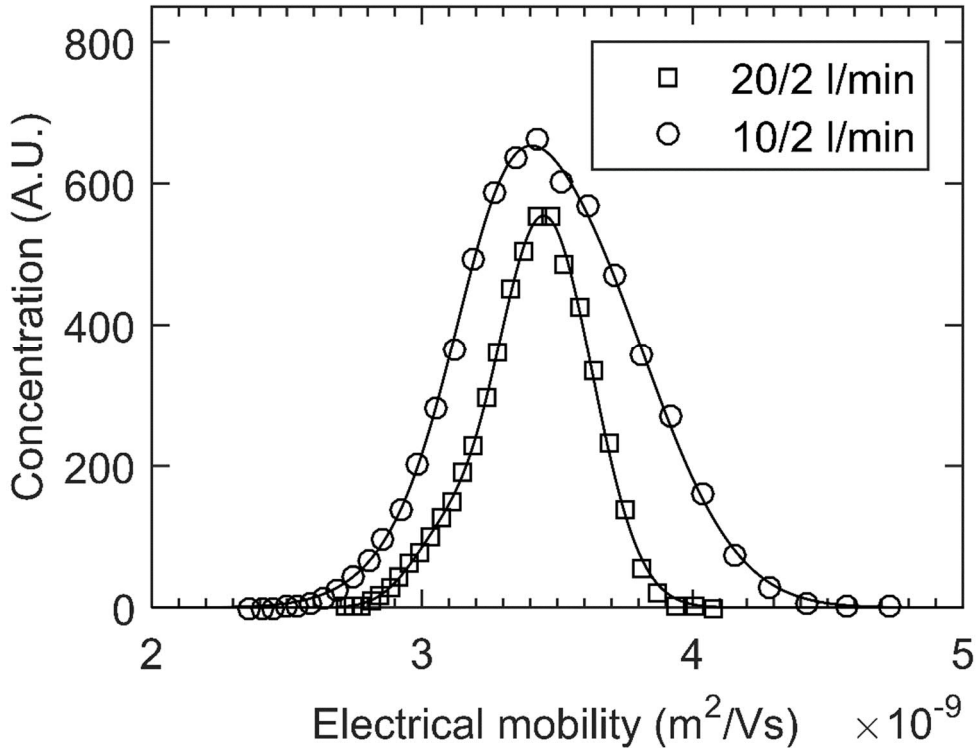

Figure 3. Tampere Long DMA transfer function for 20 l/min and 10 l/min sheath flows and 2 l/min sample flow rates.

Mixer and flow splitter tests

High quality flow splitting between the instrument under calibration and the reference instrument is essential. This was studied by measuring the bias β between two flow splitter ports including the stainless steel tubing installed after the splitter. The bias is derived for instance in Yli-Ojanperä et al. (2012) or in ISO 27891:2015. Two equal FCAEs were used as detectors in this bias measurement. First, the detection efficiency is calculated for the FCAE 2, while the FCAE 1 is considered as the reference. The detection efficiency η takes a form of

$$\eta = \frac{C_2}{C_1} = \frac{I_2}{I_1}\frac{Q_1}{Q_2}, \qquad (1)$$

where C refers to particle concentration, I is the electric current measured by the FCAE including offset correction achieved by particles on/off cycling and Q the flow rate through the FCAE. The bias β is defined through detection efficiencies by equation

$$\beta = \sqrt{\frac{\eta_a}{\eta_b}}, \tag{2}$$

where η is the detection efficiency of the instrument and the index *a* refers to the standard measurement configuration and *b* to the configuration where the flow splitter ports are switched. The inlet port switching was conducted by rotating the entire assembly containing the PTH-measurement, mixer, splitter and the inlet tubes (see Figure 1D).

The bias uncertainty is calculated from statistical Type-A factors and non-statistical Type-B factors. In this case, we take a different approach compared to the ISO 27891:2015 and evaluate the statistical uncertainty of the bias based on the differences in the calculated detection efficiencies in successive particle off-on-off repetitions in a single measurement. The statistical uncertainty of the detection efficiency $u_{Type\text{-}A}(\eta)$, is calculated from equation

$$u^2_{Type-A}(\eta) = \frac{\sum_{i=1}^{n}\left(\eta_i - \bar{\eta}\right)^2}{n(n-1)}, \tag{3}$$

where n is the number of particle on/off cycles (10) and $\bar{\eta}$ the average detection efficiency in the corresponding measurement point. This statistical Type-A uncertainty is calculated for all the measurement points and for both the normal and switched configuration separately. As a result, two series of uncertainty values are obtained, $u^2_{Type\text{-}A}(\eta_a)$ and $u^2_{Type\text{-}A}(\eta_b)$.

The non-statistical Type-B uncertainty $u_{Type\text{-}B}(\eta)$, caused by the measurement uncertainties of the instruments used, is calculated from the uncertainties of the electric current and flow measurement with equation

$$u^2_{Type-B}(\eta) = \eta^2\left(\left(\frac{u(Q_1)}{Q_1}\right)^2 + \left(\frac{u(Q_2)}{Q_2}\right)^2 + \left(\frac{u\left(\frac{I_2}{I_1}\right)}{\frac{I_2}{I_1}}\right)^2\right), \tag{4}$$

where $u(I_2/I_1)$ is the uncertainty of the proportional current measurement, $u(Q)$ the uncertainty of the flow measurement and the indices 1 and 2 refer to corresponding FCAEs. Equation 4 is calculated for all the measurement points of both the normal and switched configuration separately. Electrometer channels were calibrated twice, 4 months apart from each other, with the same current calibrator at 10 pA current. The difference in the I_2/I_1 ratio was below 0.01 % between the measurements. Because the currents measured in the actual bias measurements were lower than in the calibration, varying between 3 and 200 fA, we assigned a significantly higher standard uncertainty value of 0.25 % for the I_2/I_1 ratio than we observed in the calibrations. Flow rates Q_1 and Q_2 were controlled by mass flow controllers, which were calibrated with the same flow meter during measurements. Thus, the mass flow controller repeatability 0.1 % full scale as a standard uncertainty is considered as the measurement uncertainty (absolute accuracy is insignificant). As a consequence, the flow measurement standard uncertainty for the FCAE 1 $u(Q_1)$ is 0.002 l/min i.e. 0.14 % and for the FCAE 2 $u(Q_2)$ is 0.005 l/min i.e. 0.34 %.

The Type-A and Type-B uncertainties are combined, to obtain the total uncertainty for the detection efficiency

$$u^2(\eta) = u^2_{Type-A}(\eta) + u^2_{Type-B}(\eta). \tag{5}$$

Equations 3-5 are calculated for both configurations (a and b) and the uncertainty of the bias is calculated from

$$u(\beta)=\sqrt{\left(\frac{1}{2\eta_b}\sqrt{\frac{\eta_b}{\eta_a}}u(\eta_a)\right)^2+\left(\frac{1}{2\eta_b}\sqrt{\frac{\eta_a}{\eta_b}}u(\eta_b)\right)^2}\,, \tag{6}$$

which is multiplied by the coverage factor k=2 to obtain the expanded uncertainty expressed at a 95 % confidence level.

The concentration bias results are presented as a function of the particle diameter at 1.5 l/min flow rate in Figure 4A and as a function of the flow rate at 5.3 µm particle diameter in Figure 4B. In the whole measured particle size range, namely between 3.6 nm and 5.3 µm, the measured bias values are smaller than ±1 %, which is a very good result for such a wide particle size range. It is also worth mentioning that within the uncertainty limits, the bias value of the flow splitting is one, i.e. no bias, in the whole size range when the flow rate is 1.5 l/min. Figure 4B shows the relative concentration bias as a function of the common flow rates of the Faraday cups for 5.3 µm particles. For this largest particle size, the measured bias values range from -5.0 % to 2.1 % and show clear dependency on the flow rate. The flow mixing and splitting operates very well if the flow rate is between 1 l/min and 2 l/min for each Faraday cup. The measured bias is ±1.5 % in the range between 1 l/min and 1.75 l/min and increases slowly to 2.1 % at 2 l/min. These bias values are acceptable, as values of several percent have been reported previously (Li et al. 2014).

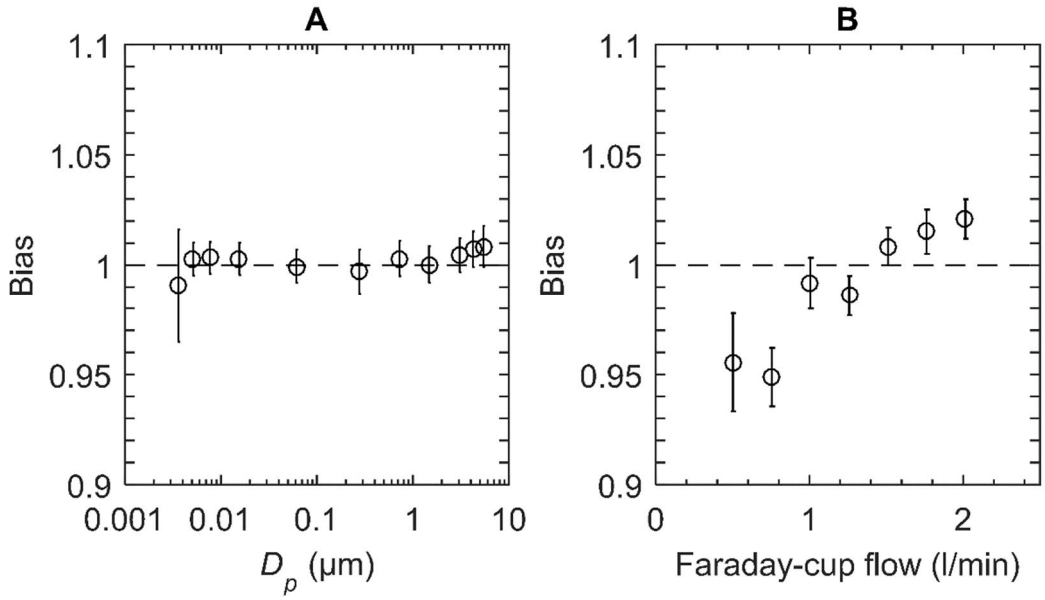

Figure 4. Flow splitter bias as a function of particle mobility diameter D_p at 1.5 l/min flow rate (A) and as a function of FCAE flow rate at 5.3 µm particle diameter (B) together with the expanded measurement uncertainties (coverage factor k=2).

CPC calibration

The detection efficiency of the CPC 3775 η_{CPC} is calculated with equation

$$\eta_{CPC}=\frac{C_{CPC}}{\beta C_{REF}}=C_{CPC}\frac{neQ\eta_{FC}}{\beta I}\,, \tag{7}$$

where C_{CPC} is the concentration measured by the CPC, C_{REF} the reference concentration from the FCAE and β the bias. The number of elementary charges per particle n is 1 because of the particle generation principle and the e is the elementary charge. The flow rate through the FCAE Q is measured by the mass flow controller including the calibration factor but it is converted to instrument inlet conditions by the aid of the pressure and temperature measurement, installed before the mixer. The electric current from the FCAE I includes the zero level correction (particle on/off measurement) and the electrometer calibration factor. The factor η_{FC} represent the FCAE detection efficiency, which is affected by diffusion losses in the case of the smallest particle sizes and by gravitational settling in the case of the largest particle sizes. The detection efficiency due diffusional loss is calculated for the inlet length of 63 mm and the flow rate of 1.5 l/min according to Gormley and Kennedy (1949). The lowest FCAE detection efficiency of 0.95 due diffusion loss is acquired for the smallest particle size of 3.6 nm. The detection efficiency due gravitational deposition in the inlet tube is calculated based on the same parameters according to Thomas (1958), and the minimum value of 0.992 is acquired for the largest particle size of 5.3 µm. The FCAE total detection efficiency is obtained by multiplying these two detection efficiency functions.

The uncertainty for the detection efficiency is evaluated for Type-A and Type-B factors. The Type-A analysis containing all the statistical factors is calculated from equation

$$u^2_{Type-A}\left(\eta_{CPC}\right) = \frac{\sum_{i=1}^{n}\left(\eta_{CPC,i} - \bar{\eta}_{CPC}\right)^2}{n\left(n-1\right)}, \tag{8}$$

in which the n is the number of cycles (10) and $\bar{\eta}$ the average detection efficiency in the corresponding measurement point.

The Type-B uncertainty is mostly related to the flow measurement accuracy, but the electrometer calibration and concentration bias are also included in the uncertainty analysis. The uncertainty of the FCAE detection efficiency was evaluated according to Yli-Ojanperä et al. (2012). In their approach, a symmetric rectangular probability distribution with a half width of 20 % of the theoretical diffusion loss (1-η_{FC}) was used for calculating the uncertainty of the detection efficiency. Now, we apply this method for the total FCAE detection efficiency, which includes both diffusion and gravitational settling. The detection efficiency uncertainty for Type-B factors takes a form of

$$u^2_{Type-B}\left(\eta_{CPC}\right) = \eta^2_{CPC}\left(\left(\frac{u\left(Q\right)}{Q}\right)^2 + \left(\frac{u\left(\eta_{FC}\right)}{\eta_{FC}}\right)^2 + \left(\frac{u\left(\beta\right)}{\beta}\right)^2 + \left(\frac{u\left(I\right)}{I}\right)^2\right), \tag{9}$$

in which $u(Q)$ is the flow measurement standard uncertainty of 0.008 l/min, i.e. 0.54 %. The flow rate is given in the instrument inlet conditions and this conversion requires pressure and temperature information. The uncertainties of temperature and pressure are small and not included in the evaluation. The values and associated uncertainty values of the bias $u(\beta)$ were taken from Figure 4. The current measurement standard uncertainty $u(I)$ is 0.06 %, except for the smallest particle size due to low particle concentration and challenging electrometer calibration at low currents 0.25 %.

The Type-A and Type-B uncertainties are combined, resulting in a total uncertainty of

$$u\left(\eta_{CPC}\right) = \sqrt{u^2_{Type-A}\left(\eta_{CPC}\right) + u^2_{Type-B}\left(\eta_{CPC}\right)}, \tag{10}$$

which is multiplied by the coverage factor k=2 in the final results to obtain expanded uncertainty at a 95 % confidence level.

The CPC 3775 counting efficiency including uncertainties is shown in Figure 5. The 50 % (lower) cut-size measured with silver particles is 5.1 nm. Hermann et al. (2007) have measured similar values for silver particles with two CPC 3775's, for one CPC approximately 4 nm and for the other one 5 nm. The particle material changes from silver to DEHS at 15 nm particle size. This 15 nm point was measured with both materials to see if there was some material dependency. However, the detection efficiencies are almost the same for both materials, 0.876±0.012 for silver and 0.881±0.012 for DEHS, which are within the uncertainty limits (k=2). When the particle size is increased, the CPC counting efficiency increases little by little peaking at 0.957 at 275 nm particle diameter. Above this, the detection efficiency begins to decrease gradually. At 1 µm particle diameter, the detection efficiency is 0.93 and drops down to 0.68 at 5.3 µm particle size. In general, the shape of the measured detection efficiency curve resembles the detection efficiency of the CPC 3772 (TSI Inc.), which has been characterized using multiple particle generation and reference methods by Yli-Ojanperä et al. (2012).

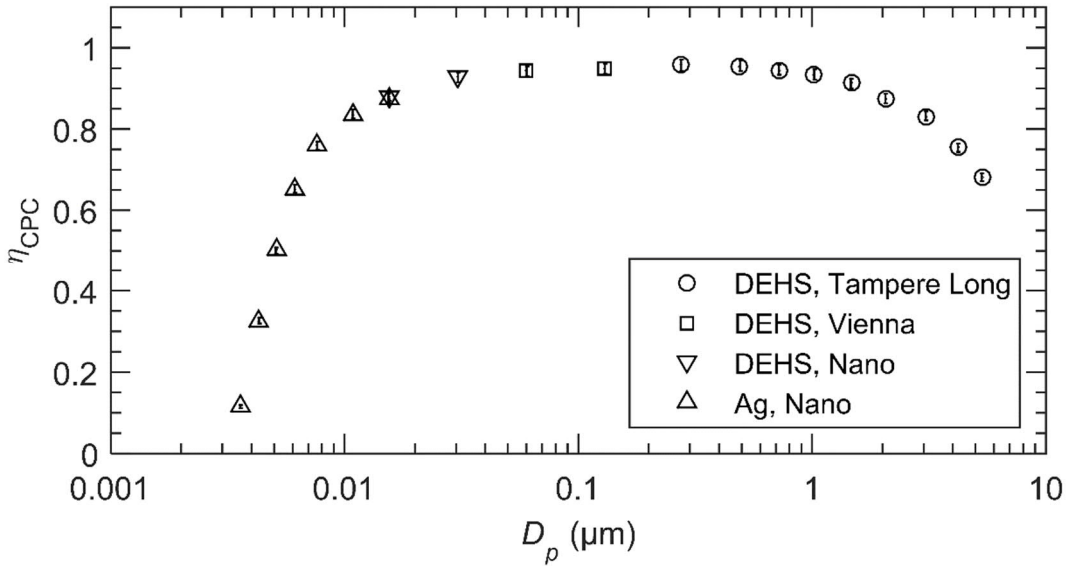

Figure 5. CPC 3775 detection efficiency η_{CPC} as a function of particle mobility diameter D_p including expanded uncertainties (k=2). The measurement point particle material and the DMA type is given in the legend.

The uncertainty components of the CPC calibration are shown in Table 1. The calibration uncertainty depends on the particle diameter. The highest expanded uncertainty value of 3.15 % (k=2) is obtained for the smallest particle size of 3.6 nm. In this case, the most significant component is the uncertainty of the flow splitter bias, which was measured at low particle concentrations and consequently at low current levels resulting in a rather low signal to noise ratio. The bias is also a significant uncertainty component at the largest particle size of 5.3 µm. However, above 5 nm particle sizes, the flow measurements produces the largest uncertainty component.

Table 1 Components of the expanded (k=2) calibration uncertainties (%) for three different particle diameters.

	Particle diameter		
Uncertainty factor	3.6 nm	720 nm	5.3 µm
Type-A uncertainty (Noise)	0.36	0.04	0.25
Bias of the flow splitting	2.61	0.73	0.91
Electrometer calibration factor	0.50	0.12	0.12
Flow rate measurement	1.07	1.07	1.07
FCAE detection efficiency	1.27	0.01	0.19
Total	**3.15**	**1.30**	**1.40**

There are some advantages in using the FCAE as a concentration reference as in our case. The main advantage of the FCAE is that the detection efficiency does not principally depend on particle size. There are diffusion losses for nanoparticles (<10 nm) and gravitational settling for large particles in the inlet tubing, but these losses may be calculated according to Gormley and Kennedy (1949) and Thomas (1958) and compensated. The large µm-sized particles experience losses in the bends of flow lines. In CPCs, the flow lines can be more complex resulting in losses for large particles. In the case of the custom made FCAE, the inlet is a short straight tube which goes directly into the detection area. Thus, the particle losses are minimal. Another advantage is that the FCAE can operate at different inlet flow rates, allowing the same flow rate to be used for the instrument under calibration and for the FCAE, which is optimal from the bias point of view.

On the down side, the FCAE cannot detect individual particles, as particle counters. This limits the lowest possible calibration concentration in the case of the FCAE acting as a reference. At 1 l/min flow rate, 1000 1/cm^3 concentration produces a current of 2.7 fA, which is low, but the calibration is still reasonable at this electric current. At the intermediate size range, the expanded uncertainty level would be less than 2 % in this case, if the other uncertainty factors than the signal to noise ratio, and the electrometer calibration factor remained constant. The calibration concentration could be reduced to some extend, perhaps down to 200 1/cm^3, if the measurement time was increased. If the number of cycles was tripled, resulting in a total calibration time of 122 min, the expanded uncertainty would be less than 3 % at 1 l/min FCAE flow rate. Another option would be to utilize the bipolar calibration routine (Pihlava et al. 2016), which increases the signal to noise ratio of the electrical measurement.

Conclusions

We have introduced an aerosol instrument calibration setup based on the work by Uin et al. (2009) and Yli-Ojanperä et al. (2010) with an exceptionally wide particle size range. The setup relies on production of singly charged particles, allowing both size and concentration calibrations. The FCAE is used as a concentration reference, which allows definition of a traceable particle concentration through electric current and flow rate measurements in a wide size range. The advantages, in addition to the wide size range, are that a single particle generator covers the whole particle size range and that the particle size selection is straightforward using DMAs. The size is selected by adjusting correct saturator temperature and correct DMA settings, including selection of the DMA. As commercial DMAs have limited

size ranges, a new DMA, was developed for µm-sized particles. Previously (e.g. Yli-Ojanperä et al. 2012), multiple, completely different particle generation methods and different concentration references have been required to cover the size range, which is now possible with the new setup.

The operation of the main components was tested. The particle size as a function of the growth unit saturator temperature was measured. The transfer function of the constructed Tampere Long DMA was also measured. The transfer function was not completely triangular with 20 l/min sheath and 2 l/min sample flows but the resolution of the DMA was still 7.95. In the number concentration calibrations, the flow splitting between the instrument and reference is important. To this end, a new flow mixing and splitting setup was designed and constructed. We measured the flow splitter bias with two identical FCAEs at equal inlet flow rates as a function of the flow rates, and observed some dependency on the flow rate at 5.3 µm particle size. The bias was also studied as a function of the particle size between 3.6 nm and 5.3 µm at 1.5 l/min inlet flow rates. The measured bias values were found to be smaller than ±1 % in the whole measured particle size range at 1.5 l/min flow rate.

The setup was applied in an example calibration of the CPC detection efficiency from 3.6 nm to 5.3 µm. The size range of the developed setup was wide enough to define the cut diameter of 5.1 nm and to see the decrease in the counting efficiency for over 1 µm particle sizes. The expanded uncertainties (k=2) of the detection efficiencies were less than 4 % over the entire size range and less than 2 % between 5 nm and 5.3 µm. The smallest particle sizes are associated with the largest uncertainties, because of low particle concentrations in both bias and CPC calibration measurements, which affect especially the uncertainty of the bias. Above 5 nm particle size, the most significant uncertainty factor is the flow measurement.

In summary, the developed calibration setup is relatively easy to use and based on the example CPC calibration it suits very well for the calibration of various CPCs and other aerosol instruments. As a comparison to other available methods in the µm-size range, the calibration concentrations of the developed setup are relatively high, approximately 15000 1/cm^3 at 2 µm particle size and over 2500 1/cm^3 at 5.3 µm particle size, which allows calibration of low sensitivity instruments. The future tasks are to enhance the calibration setup size accuracy by calibrating classification DMAs against multiple reference sizes and to estimate the uncertainty for the output size.

Acknowledgements

The authors gratefully acknowledge support from the MMEA research program of the Cluster for Energy and Environment (CLEEN Ltd.), funded by Tekes - the Finnish Funding Agency for Technology and Innovation. Authors thank Antti Lepistö, Veli-Pekka Plym and Timo Lindqvist for manufacturing the calibration setup components.

References

Berglund, R. N., and Liu, B. Y. H. (1973). Generation of Monodisperse Aerosol Standards. Environ. Sci. Technol., 7:147-153.

CEN/TS 16976:2016. Ambient air - Determination of the particle number concentration of atmospheric aerosol.

Duan, H, Romay, F.J., Li, C., Naqwi, A., Deng, W., and Liu, B.Y.H. (2016). Generation of monodisperse aerosols by combining aerodynamic flow-focusing and mechanical perturbation. *Aerosol Sci. Technol.*, 50:17-25.

European Commission (2008). Commission Regulation (EC) No 692/2008 of 18 July 2008 implementing and amending Regulation (EC) No 715/2007 of the European Parliament and of the Council on type-approval of motor vehicles with respect to emissions from light passenger and commercial vehicles (Euro 5 and Euro 6) and on access to vehicle repair and maintenance information. *Official Journal of the European Union*, L 199.

Fletcher, R. A., Mulholland G. W., Winchester M. R., King, R. L., and Klinedinst, D. B. (2009). Calibration of a Condensation Particle Counter Using a NIST Traceable Method. *Aerosol Sci. Technol.*, 43:425-441.

Fuchs, N. A. (1963). On the stationary charge distribution on aerosol particles in a bipolar ionic atmosphere. *Geofis. pura appl.*, 56:185-193.

Gormley, P. G., and Kennedy, M. (1949). Diffusion from a Stream Flowing through a Cylindrical Tube. *Proc. R. Irish Acad.*, 52(A):163-169.

Gupta, R., and McFarland, A.R. (2001). Experimental Study of Aerosol Deposition in Flow Splitters with Turbulent Flow. *Aerosol Sci. Technol.*, 34:216-226.

Hermann, M., Wehner, B., Bischof, O., Han, H.-S., Krinke, T., Liu, W., Zerrath, A., and Wiedensohler, A. (2007). Particle counting efficiencies of new TSI condensation particle counters. *J. Aerosol Sci.*, 38, 674-682.

Hillamo, R., and Kauppinen E. (1991) On the Performance of the Berner Low Pressure Impactor. *Aerosol Sci. Technol*, 14:33-47.

Högström, R., Yli-Ojanperä, J., Rostedt, A., Iisakka, I., Mäkelä, J. M., Heinonen, M., and Keskinen, J. (2011). Validating the single charged aerosol reference (SCAR) as a traceable particle number concentration standard for 10 nm to 500 nm aerosol particles. *Metrologia*, 48:426-436.

Högström, R., Quincey, P., Sarantaridis, D., Lüönd, F., Nowak, A., Riccobono, F., Tuch, T., Sakurai, H., Owen, M., Heinonen, M., Keskinen, J., and Yli-Ojanperä, J. (2014). First comprehensive inter-comparison of aerosol electrometers for particle sizes up to 200 nm and concentration range 1000 cm−3 to 17 000 cm−3. *Metrologia*, 51:293-303.

Iida, K., Sakurai, H., Saito, K., and Ehara, K. (2014). Inkjet Aerosol Generator as Monodisperse Particle Number Standard. *Aerosol Sci. Technol.*, 48:789-802.

ISO 14644-1:2015 Cleanrooms and associated controlled environments -- Part 1: Classification of air cleanliness by particle concentration

ISO 27891:2015. Aerosol particle number concentration – Calibration of condensation particle counters.

Järvinen, A., Heikkilä, P., Keskinen J., and Yli-Ojanperä, J. (2014). Particle charge-size distribution measurement using a differential mobility analyzer and an electrical low pressure impactor. *Aerosol Sci. Technol.*, 51:20-29.

Kauppinen, E. I., Hillamo, R. E. (1989). Modification of the University of Washington Mark 5 in-stack impactor. *J. Aerosol Sci.*, 20:813-827.

Keskinen, J., Pietarinen, K., and Lehtimäki, M. (1992). Electrical Low Pressure Impactor. *J. Aerosol Sci.*, 23:353-360.

Keskinen, J., Marjamäki, M., Virtanen, A., Mäkelä, T., Hillamo, R. (1999). Electrical calibration method for cascade impactors. *J. Aerosol Sci.*, 30:111-116.

Kimoto, S., Dick, W.D., Hunt, B., Szymanski, W.W., McMurry P.H., Roberts, D.L., and Pui, D. Y. H. (2017). Characterization of nanosized silica size standards. *Aerosol Sci. Technol.*, 51:936-945.

Knutson, E. O., and Whitby, K. T. (1975). Aerosol classification by electric mobility: apparatus, theory, and applications. *J. Aerosol Sci.*, 8:443-451.

Li, L., Mulholland, G. W., Windmuller, L., Owen, M. C., Kimoto, S., and Pui, D. Y. H. (2014). On the Feasibility of a Number Concentration Calibration Using a Wafer Surface Scanner. *Aerosol Sci. Technol.*, 48:747-757.

Liu, B. Y. H., and Pui, D. Y. H. (1974). A Submicron Aerosol Standard and Primary, Absolute Calibration of the Condensation Nuclei Counter. *J. Coll. Interf. Sci.*, 47:156-171.

Marjamäki, M., Keskinen, J., Chen, D-R., and Pui, D.Y.H. (2000). Performance evaluation of electrical low pressure impactor (ELPI). *J. Aerosol Sci.*, 31:249-261.

Marple, V. A., Rubow, K. L., Behm, S. M. (1991) A Microorifice Uniform Deposit Impactor (MOUDI): Description, Calibration, and Use. *Aerosol Sci. Technol.*, 14:434-446.

Owen, M., Mulholland, G., and Guthrie, W. (2012). Condensation Particle Counter Proportionality Calibration from 1 Particle·cm^{-3} to 10^{4} Particles·cm^{-3}. *Aerosol Sci. Technol.*, 46:444-450.

Pihlava, K., Keskinen, J., and Yli-Ojanperä, J. (2016). Improving the signal-to-noise ratio of Faraday cup aerosol electrometer based aerosol instrument calibrations. *Aerosol Sci. Technol.*, 50-373-379.

Romay-Novas, F., and Pui, D.Y.H. (1988). Generation of Monodisperse Aerosols in the 0.1-1.0-μm Diameter Range Using a Mobility Classification-Inertial Impaction Technique. *Aerosol Sci. Technol.*, 9:123-131.

Sinclair, D., and La Mer, V. K. (1948). Light scattering as a measure of particle size in aerosols. *Chemical Reviews*, 44:245-267.

Thomas, J. W. (1958). Gravity Settling of Particles in a Horizontal Tube. *J. Air Pollut. Control Assoc.*, 8:32-34.

Uin, J., Tamm, E., and Mirme, A. (2009). Electrically Produced Standard Aerosols in a Wide Size Range. *Aerosol Sci. Technol.*, 43:847-853.

Uin, J., Tamm, E., and Mirme, A. (2011). Very Long DMA for the Generation of the Calibration Aerosols in Particle Diameter Range up to 10 μm by Electrical Separation. *Aerosol Air Qual. Res.*, 11:531-538.

Wiedensohler, A. (1988). An approximation of the bipolar charge distribution for particles in the submicron size range. *J. Aerosol Sci.*, 19:387-389.

Winklmayr, W., Reischl, G.P., Lindner, A.O., and Berner, A. (1991). A new electromobility spectrometer for the measurement of aerosol size distributions in the size range from 1 to 1000 nm. *J. Aerosol Sci.*, 22:289-296.

Yli-Ojanperä, J., Mäkelä, J.M., Marjamäki, M., Rostedt, A., and Keskinen, J. (2010). Towards Traceable Particle Number Concentration Standard: Single Charged Aerosol Reference (SCAR). *J. Aerosol Sci.*, 41:719-728.

Yli-Ojanperä, J., Sakurai, H., Iida, K., Mäkelä, J., Ehara, K., and Keskinen, J. (2012). Comparison of Three Particle Number Concentration Calibration Standards Through Calibration of a Single CPC in a Wide Particle Size Range. *Aerosol Sci. Technol.*, 46:1163-1173.

Yli-Ojanperä, J., Ukkonen, A., Järvinen, A., Layzell, S., Niemelä, V., and Keskinen, J. (2014). Bipolar Charge Analyzer (BOLAR): A New Aerosol Instrument for Bipolar Charge Measurements. *J. Aerosol Sci.*, 77:16-30.